Biotechnology and Bioprocess Engineering 22: 637-646 (2017)
DOI 10.1007/s12257-017-0121-4

pISSN 1226-8372
eISSN 1976-3816

RESEARCH PAPER

Chemical Characterization of Dissolved Organic Matter in Moist Acidic Tussock Tundra Soil Using Ultra-high Resolution 15T FT-ICR Mass Spectrometry

Jung Hoon Choi, Yun-Gon Kim, Yoo Kyung Lee, Seung Pil Pack, Ji Young Jung, and Kyoung-Soon Jang

Received: 29 March 2017 / Revised: 18 August 2017 / Accepted: 18 September 2017

Abstract Global warming is considered one of the most serious environmental issues, substantially mediating abrupt climate changes, and has stronger impacts in the Arctic ecosystems than in any other regions. In particular, thawing permafrost in the Arctic region with warming can be strongly contributing the emission of greenhouse gases (CO_2 and CH_4) that are produced from microbial decomposition of preserved soil organic matter (SOM) or are trapped in frozen permafrost soils, consequently accelerating global warming and abrupt climate changes. Therefore, understanding chemical and physical properties of permafrost SOM is important for interpreting the chemical and biological decomposability of SOM. In this study, we investigated dissolved organic matter (DOM) along the soil depth profile in moist acidic tussock tundra to better understand elemental compositions and distributions of the arctic SOM to evaluate their potential decomposability under climate change. To achieve ultra-high resolution mass profiles, the soil extracts were analyzed using a 15 Tesla Fourier transform ion cyclotron resonance mass spectrometer in positive and negative ion modes *via* electrospray ionization. The results of this analysis revealed that the deeper organic soil (2Oe1 horizon) exhibits less CHON class and more aromatic class compounds compared to the surface organic soils, thus implying that the 2Oe1 horizon has undergone a more decomposition process and consequently possessed the recalcitrant materials. The compositional features of DOM in the Arctic tundra soils are important for understanding the changes in biogeochemical cycles caused from permafrost changes associated with global warming and climate change.

Keywords: dissolved organic matter, FT-ICR MS, arctic tundra soil, elemental composition, decomposability

1. Introduction

The Arctic permafrost represents a large carbon reservoir that contains one third of the global soil carbon budget, thus considerably affecting global ecosystem [1]. The amount of organic carbon stored in northern arctic permafrost is approximately 1,700 Pg that is regarded as twice as much as in the atmosphere, and most of the soil organic carbon (88% of the total) remains frozen all year round [2,3]. Global warming that is substantially caused by increased greenhouse gas emissions (*i.e.*, CO_2 and CH_4) has led to permafrost thaw, being associated with the mobilization of

---

Jung Hoon Choi, Kyoung-Soon Jang*
Biomedical Omics Group, Korea Basic Science Institute, Cheongju 28119, Korea
Tel: +82-43-240-5196; Fax: +82-43-240-5158
E-mail: ksjang@kbsi.re.kr

Jung Hoon Choi, Seung Pil Pack
Department of Biotechnology and Bioinformatics, Korea University, Sejong 30019, Korea

Yun-Gon Kim
Department of Chemical Engineering, Soongsil University, Seoul 06978, Korea

Yoo Kyung Lee, Ji Young Jung*
Division of Life Sciences, Korea Polar Research Institute, KIOST, Incheon 21990, Korea
Tel: +82-32-760-5532; Fax: +82-32-760-5534
E-mail: jyjung@kopri.re.kr

Kyoung-Soon Jang
Department of Bio-Analytical Science, University of Science and Technology, Daejeon 34113, Korea

ancient dissolved organic matter (DOM) from deeper horizons to top surfaces [4]. Furthermore, the permafrost thaw facilitates microbial decomposition of organic carbons in arctic permafrost soils, then consequently accelerates the release of greenhouse gases [5-7]. Therefore, environmental researchers have paid much attention to the changes in carbon dynamics of northern circumpolar regions associated with global warming and abrupt climate change.

Soil organic matter (SOM) is often considered as a repertoire of biologically and chemically-processed organic carbon species, reflecting soil microbial diversity, activity and nutrient cycling so that the chemical compositions of SOM vary by location, depth and climate [8,9]. There are several factors affecting SOM stabilization or decomposition; chemical recalcitrance of SOM, mineral association, and accessibility of decomposers to SOM [10]. Among those, chemical recalcitrance is the basic feature to determine the decomposability of SOM; however, the compositional characteristics and chemical property of SOM remain challenging because SOM consists of heterogeneous C sources with a variety of compositions, ranging from simple sugars, organic acids, and amino acids to more complex polymers such as cellulose, lignin, and lignocellulose, and structural characteristics (*i.e.,* degrees of polymerization and aromaticity). Therefore, the elucidation of chemical compositions and distributions of SOM is the first step to better understand the impacts of global warming and climate changes on the arctic permafrost soil changes.

Several approaches have been used to characterize the chemical composition of organic matter in soils [11,12]. One of the simplest methods is analyzing and quantifying elemental compositions in soils (*i.e.,* carbon, nitrogen and phosphorus) using an elemental analyzer. The other approaches are measuring the amount of a specific class of compounds present in SOM using selective extraction methods, such as the organic solvent-based extraction for lipids and the CuO oxidation for lignins [13]. Various spectroscopic techniques [Fourier transform infrared (FTIR), ^{13}C nuclear magnetic resonance (NMR), UV-Vis and excitation-emission matrix (EEM) fluorescence] have also been widely used to characterize water and soil-derived organic matter [14-17]; however, those spectroscopic methods only provide information about the functional groups of SOM but not the individual components. Recently, pyrolysis-gas chromatography mass spectrometry (pyGC-MS) has been used for identifying soil organic compounds and understanding their compositional changes [18,19], but even this technique is insufficient for resolving complex constituents.

Fourier transform ion cyclotron resonance mass spectrometry (FT-ICR MS) has emerged as a powerful tool for the analysis of extremely complex mixtures, such as crude oils, water and soil-derived organic substances, resulting in rapid and accurate interpretation of the elemental compositions of complicated samples [20-25]. From the highly accurate mass data acquired by using FT-ICR MS, the assignment of elemental compositions based on exact mass differences is made, then the assigned formulas are sorted by chemical class, double bond equivalent and carbon number. The formula assignment can be possible because the natural organic matter (NOM) is mainly composed of C, H and O elements, and less frequently with N and S. Other trace elements could be ignored for the interpretation of elemental compositions of SOM. Overall, the unsurpassed resolving power (full width at half maximum, FWHM: >400,000) and mass accuracy (<1 ppm) of FT-ICR MS and the development of advanced data processing tools and graphical methods has made it possible to successfully identify the chemical compositions of extremely complicated samples [20,26,27]. Recently, high-field FT-ICR MS was used to study DOM in permafrost soils [4,28].

Permafrost soil consists of the active layer, which experiences seasonal thawing and freezing repeatedly, and the permafrost layer, which stays in a frozen state throughout the whole year. Our study site, Council, Alaska is located in subarctic zone that is very vulnerable to climate change. Moreover, thermokarst formation would be extended with warming, and thereby the export of old DOM preserved in a deeper soil layer could be facilitated with permafrost thaw. Diversity and distribution of DOM in arctic tundra soils are also influenced by vegetation types and soil microbial community structure, influencing nutrient concentrations, decompositions and pools of carbon and nitrogen sources [29-31]. In this study, we investigated the chemical composition of DOM in moist acidic tussock tundra soils from active to permafrost layers using an ultra-high resolution 15T FT-ICR MS. The resulting data were interpreted to investigate the characteristics of the tundra soils. This approach would open our insights toward changes on the Arctic soils regarding climate changes.

2. Materials and Methods

2.1. Soil sampling

Soil core sampling was conducted as described previously in moist acidic tussock tundra [32]. Briefly, a soil core was collected using a SIPRI corer into the permafrost (up to 1.5 m) in Council, Alaska (64° 51′N, 163° 42′W), then stored at -20°C prior to use.

2.2. Extraction of dissolved organic matter from the arctic tundra soils

Soils, taken from a depth of 0 ~ 5 cm (Oe horizon, surface

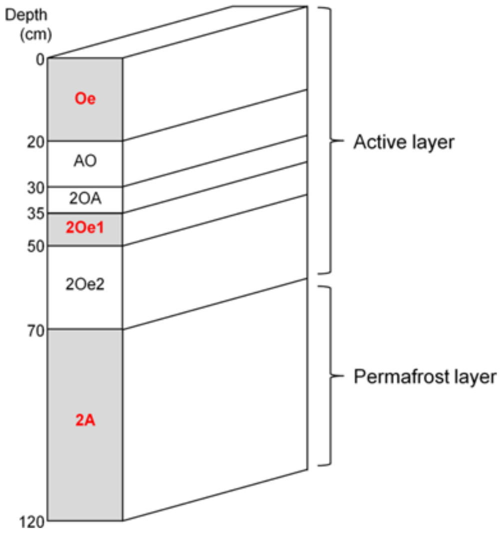

Fig. 1. Composition of soil layers in the moist acidic tussock tundra. The soil was classified as Typic Histoturbels because of the characteristics of Histoturbels with a deep organic layer and cryoturbated organic materials in between mineral soils and the soil horizon was separated by O (organic materials) and A (sand and silt) based on the soil texture followed by UDSA scheme from USDA Soil Taxonomy [46].

organic soil), 35 ~ 40 cm (2Oe1 horizon, deeper organic soil) and 70 ~ 75 cm (2A horizon, mineral soil), as shown in Fig. 1, were air dried, ground using a mortar and pestle, and passed through a 2 and 0.475 mm sieve. The resulting tundra soils (each 100 mg) were transferred to sterile amber glass vials (Wheaton, Millville, NJ), extracted with 1 mL of ultrapure water in an ultrasonic bath for 2 h, and filtered with a 0.45 µm Teflon syringe filter to remove insoluble particles. The filtrates were acidified to pH 2 using 1 M HCl, then loaded on an Oasis HLB cartridge (Waters, Milford, MA) to remove inorganic constituents. DOM of the tundra soil samples was retained on the cartridge and eluted with 1.5 mL of methanol containing 2% ammonium hydroxide solution. The resulting eluates were immediately evaporated to dryness under a gentle nitrogen stream and redissolved with 50% aqueous methanol containing 0.1% formic acid for FTMS analysis with positive ion mode. For negative ion mode analysis, it was reconstituted with 50% aqueous methanol containing 7% ammonium hydroxide solution.

2.3. FT-ICR MS analysis

Ultra-high resolution MS analyses were performed on a 15T FT-ICR mass spectrometer equipped with an electrospray ionization (ESI) source (solariX^{TM} system, Bruker Daltonics, Billerica, MA) in Korea Basic Science Institute. The DOM samples were directly infused into the 15T FT-ICR mass spectrometer with a syringe pump at a flow rate of 3 µL/min. A mass resolving power of greater than 500,000 (at *m/z* 400) was routinely achieved for all spectra while collecting 200 scans per sample with a 4 M transient. The other MS parameters were as follows: capillary voltages of ± 3,900 V, drying gas flow rates of 4 L/min, drying gas temperatures of 180°C, an ion accumulation time of 0.05 sec and a transient length of 1.39 sec. External calibration was performed with quadratic regression using an arginine solution (10 µg/mL in methanol). The data acquisition was controlled by ftmsControl 2.0 software (Bruker Daltonics).

2.4. Data processing and elemental composition assignments

Raw data obtained from the 15T FT-ICR MS analyses were processed using DataAnalysis (ver. 4.2, Bruker Daltonics) and Composer (Sierra Analytics, Modesto, CA) software, as described previously [33] with some modifications. After 15T FT-ICR MS measurements, the raw spectra were imported to the DataAnalysis 4.2 for peak detection and recalibration. Composer, a formula calculator, was employed to assign elemental compositions, as described previously [34], with some modifications. Briefly, the empirical molecular formulas were calculated for the masses of singly charged ions in the range of *m/z* 150 ~ 1,100 by combinations of up to 100 ^{12}C, 200 ^{1}H and 50 ^{16}O atoms, followed by additional calculations of molecular formula including up to 2 ^{14}N and 1 ^{32}S atoms, as described by Koch *et al.* [35]. Then, the molecular formulas with assignment errors of > 0.5 ppm and those found from blank extracts were excluded from further processing. A van Krevelen plot was used to visualize the assigned compositions of the samples based on their molar H/C and O/C ratios [27].

3. Results and Discussion

3.1. Ultra-high resolution FT-ICR MS analysis of DOM from moist acidic tussock tundra soils

To investigate the molecular profile of DOM in moist acidic tussock tundra soil in Council, Alaska, samples were collected from top surface soils to deeper permafrost soils, as described in our previous study [32]. The collected soil core was composed of Oe (sapric, partially decomposed) horizon on the top, AO or OA, and 2Oe horizons in the active layer, and the permafrost layer did not include any organic horizon and consisted with mineral materials, A horizon (Fig. 1). Both Oe (surface organic) and 2Oe (deeper organic) horizons were composed of hemic materials, but may vary with the source, formation time, *etc.* The 2A horizon in the permafrost seemed different from the A horizon in the active layer either. The situated soil samples for the DOM analysis were used to extract DOM with

Table 1. Property comparison of the assigned compositions of soil organic matter, extracted from moist acidic tussock tundra soils

Sample		# Of assigned peaks	DBE^{*}_{ave}	Average compositions			
				O/C	H/C	N/C (C/N)	S/C
Positive mode	Oe (0 ~ 5 cm)	3,000	6.64	0.31	1.57	0.06 (16.7)	0.0014
	2Oe1 (35 ~ 40 cm)	3,285	7.13	0.29	1.50	0.02 (50)	0.0010
	2A (70 ~ 75 cm)	3,684	6.68	0.28	1.49	0.04 (25)	0.0016
Negative mode	Oe (0 ~ 5 cm)	3,085	6.80	0.39	1.39	0.07 (14.3)	0.0018
	2Oe1 (35 ~ 40 cm)	3,165	8.09	0.37	1.23	0.03 (33.3)	0.0003
	2A (70 ~ 75 cm)	2,904	7.24	0.39	1.26	0.05 (20)	0.0020

*The double bond equivalent (DBE) value representing the sum of rings and double bonds in each molecule can be calculated from the number of atoms in chemical formulae by the following equation: $DBE=1+C-H/2+N/2$.

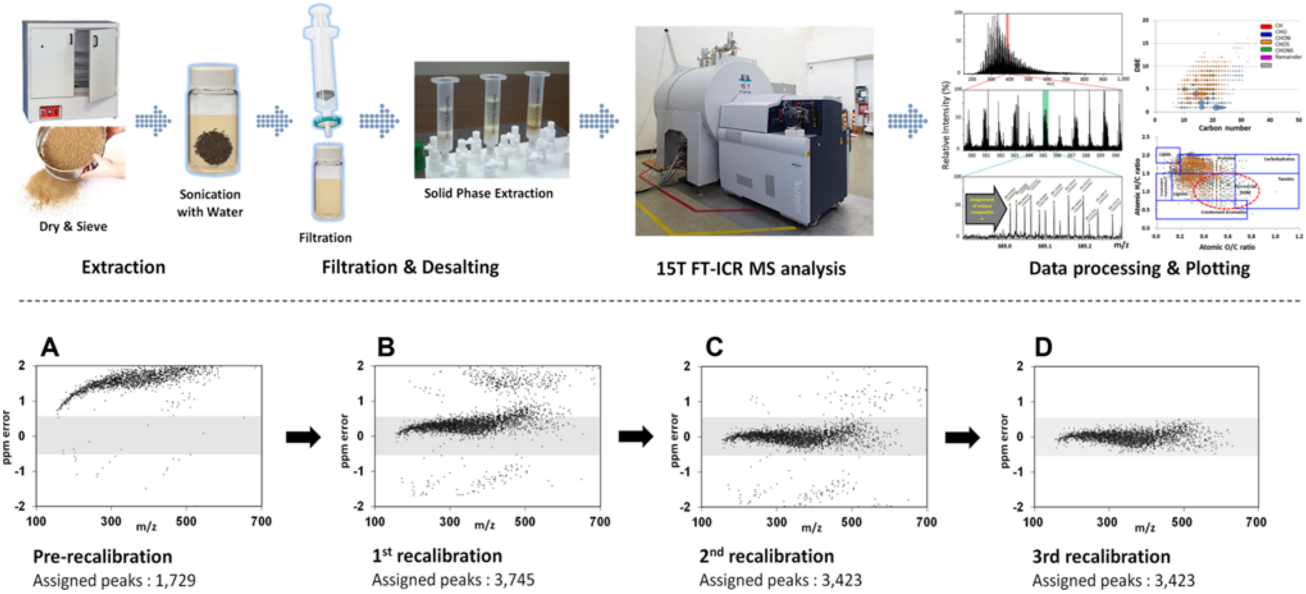

Pre-recalibration
Assigned peaks : 1,729

1st recalibration
Assigned peaks : 3,745

2nd recalibration
Assigned peaks : 3,423

3rd recalibration
Assigned peaks : 3,423

Fig. 2. Schematic diagram of the soil organic matter analysis using ultra-high resolution FT-ICR MS. The lower panel shows the recalibration process of the FTMS data for the assignment of molecular formulae. After the 3rd recalibration of the FTMS spectra was done, 3,423 molecular formulas were assigned within 0.5 ppm error (D), whereas 1,729 molecules were assigned and all the peaks were beyond the error range before the recalibration (A).

water. The Oe and 2A horizons contained the highest and the lowest total carbon content, respectively. The deeper organic horizon (2Oe) showed completely different chemical properties compared to the surface organic horizon (Oe). All chemical properties of the soil samples including pH, total carbon (TC) and total nitrogen (TN) contents, and C/N ratio that were obtained in our previous study [32], were summarized in Supplementary Table 1.

Soil extracts were then analyzed using an ultra-high resolution 15T FT-ICR mass spectrometer equipped with ESI source, as described in Fig. 2. The ultra-high resolution FT-ICR MS analysis was applied with both positive and negative ion modes to obtain a more complete description of the molecular composition of the arctic DOM [36]. As shown in Figs. 3 and 4, the FTMS spectra of the soil extracts appear to differ by the ionization modes. The mass spectra obtained from a blank extract were used as the control. After processing the raw DOM data using Composer software, 5,305 and 4,538 molecular formulas were assigned to the ESI (+) and (-) FT-ICR MS data, respectively. All chemical characteristics of the assigned elemental formulae that were calculated using the Composer software from the

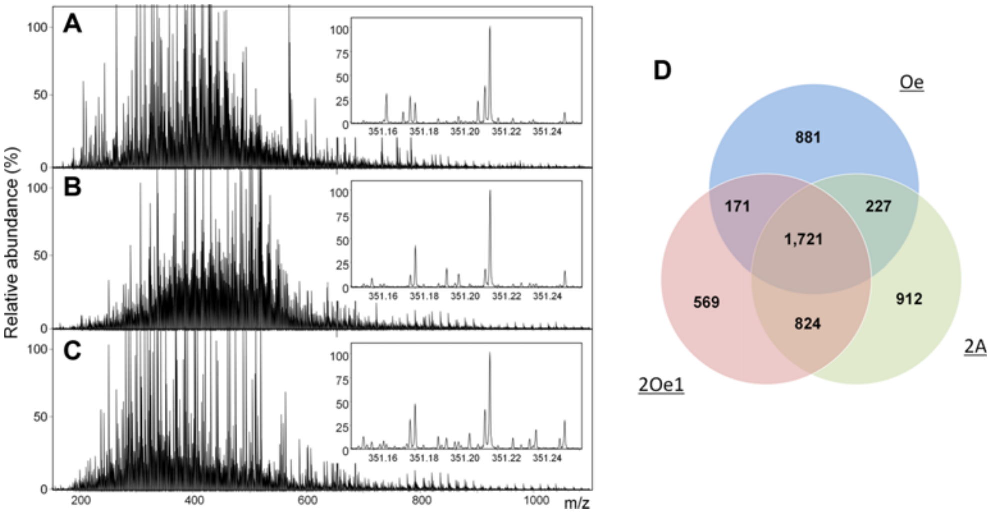

Fig. 3. Ultra-high resolution 15T FT-ICR MS analysis of arctic tundra soil extracts. FTMS spectra of (A) Oe, (B) 2Oe1, and (C) 2A extracts, obtained *via* ESI (+). The insets represent the assigned peaks for a nominal mass of *m/z* 351. (D) Venn diagram representing the relationships among the sets of elemental formulas that were calculated from the raw data for Oe, 2Oe1 and 2A extracts.

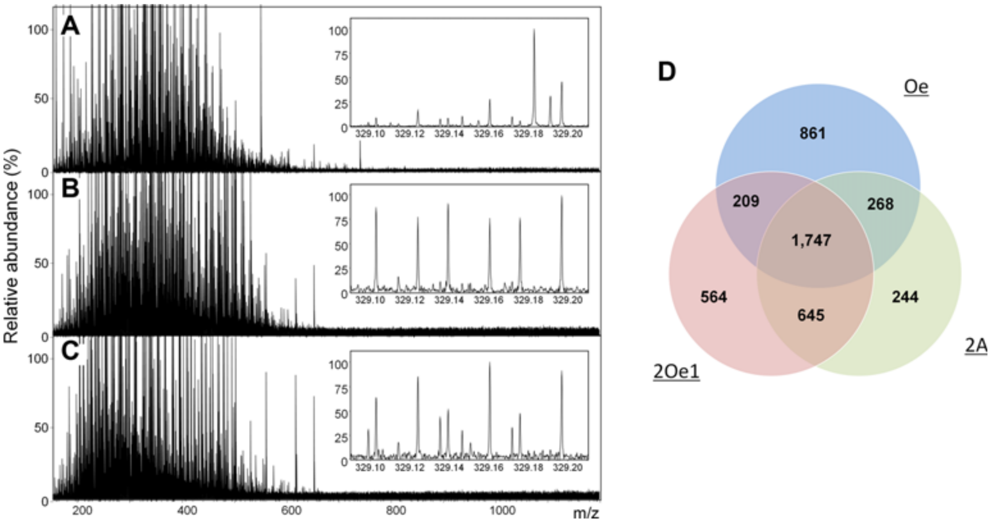

Fig. 4. Ultra-high resolution 15T FT-ICR MS analysis of arctic tundra soil extracts. FTMS spectra of (A) Oe, (B) 2Oe1, and (C) 2A extracts, obtained *via* ESI (-).The insets represent the assigned peaks for a nominal mass of *m/z* 329. (D) Venn diagram representing the relationships among the sets of elemental formulas that were calculated from the raw data for Oe, 2Oe1, and 2A extracts.

FTMS data of tundra SOM were listed in Supplementary Table 2. The Venn diagrams in Figs. 3D and 4D demonstrate the relationships among the sets of elemental formulas. The insets in Figs. 3 and 4 represent the selected regions of the FTMS spectra showing the differences depending on the soil depths and types. The overall chemical attributions of the organic compounds included in the Oe, 2Oe1, and 2A extracts are summarized in Table 1.

3.2. Compositional differences in tundra SOM depending on the soil depth

To understand the molecular characteristics of the arctic SOM, the chemical compositions and class distributions of the Oe, 2Oe1 and 2A extracts were visualized using pie charts and van Krevelen diagrams (Figs. 5 and 6). ESI (+) FTMS analysis revealed that CHON class compounds were abundant in the Oe extract (67.5% of the total based on the relative ion intensity), whereas the CHON class species were 44.6 and 51.1% of the totals in the 2Oe1 and 2A extracts, respectively. In contrast, CHO class compounds occupied 30% of the total in the Oe, but exhibited increased aspects in the 2Oe1 (53.3% of the total) and 2A (45.7% of the total) horizons. The results of ESI (-) FTMS analysis are consistent with the ESI (+) data, but the percentage of

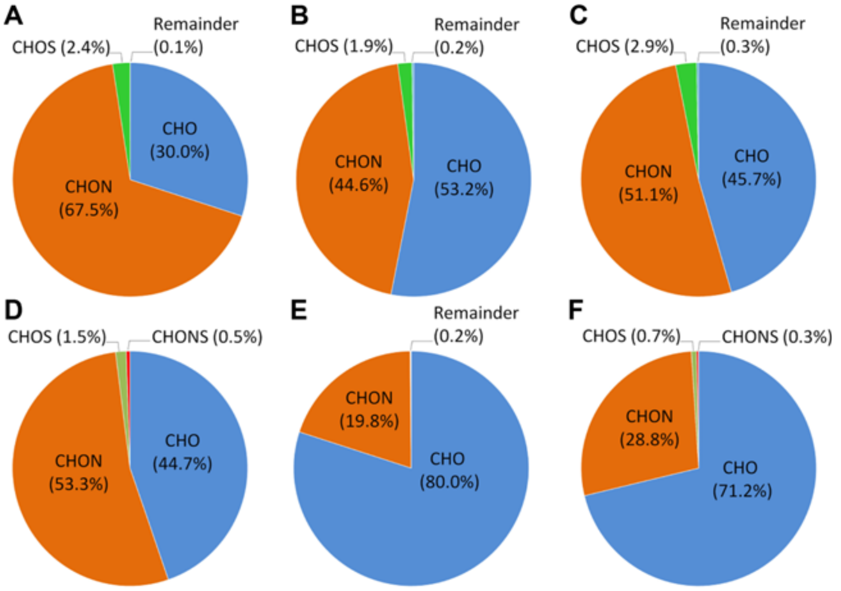

Fig. 5. Venn diagrams representing the relationships among the sets of elemental formulas that were calculated from the raw data for Oe (A and D), 2Oe1 (B and E), 2A (C and F) extracts, analyzed by ESI (+) [A-C] and (-) [D-F] FT-ICR MS.

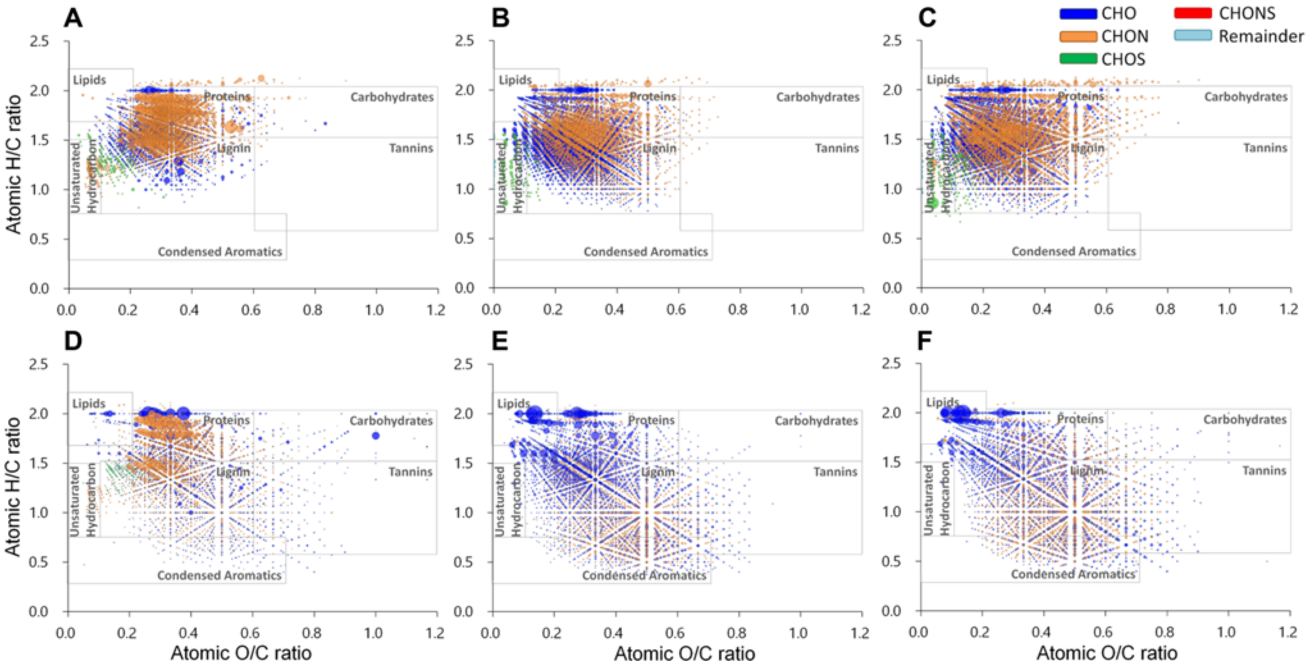

Fig. 6. Van Krevelen diagrams showing the molar H/C and O/C ratios of assigned elemental compositions from arctic tundra soil extracts, analyzed by ESI (+) and (-) FT-ICR MS (color code: CH, red; CHO, blue; CHON, orange; CHOS, green; CHONS, purple; Remainder, gray). (A) Oe, (B) 2Oe1, and (C) 2A were analyzed *via* ESI (+), while (D) Oe, (E) 2Oe1, and (F) 2A were analyzed *via* ESI (-).

the CHO compounds were much greater than those from the ESI (+) data, assuming the O-containing compounds in the tundra DOM possess hydroxyl or carboxyl functional groups that are prone to ionizing in negative ion mass spectra. The expanded FTMS spectra at the nominal mass of 351 (for positive ion mass spectra) and 329 (for negative ion mass spectra) showed that N-containing compounds disappeared significantly in the 2Oe1 horizon compared with the Oe horizon, supporting the significant reduction of CHON compounds in the deeper organic soils at a molecular level (Fig. 7). Fast decomposition of SOM in the moist acidic tundra may be constrained by the lower soil N

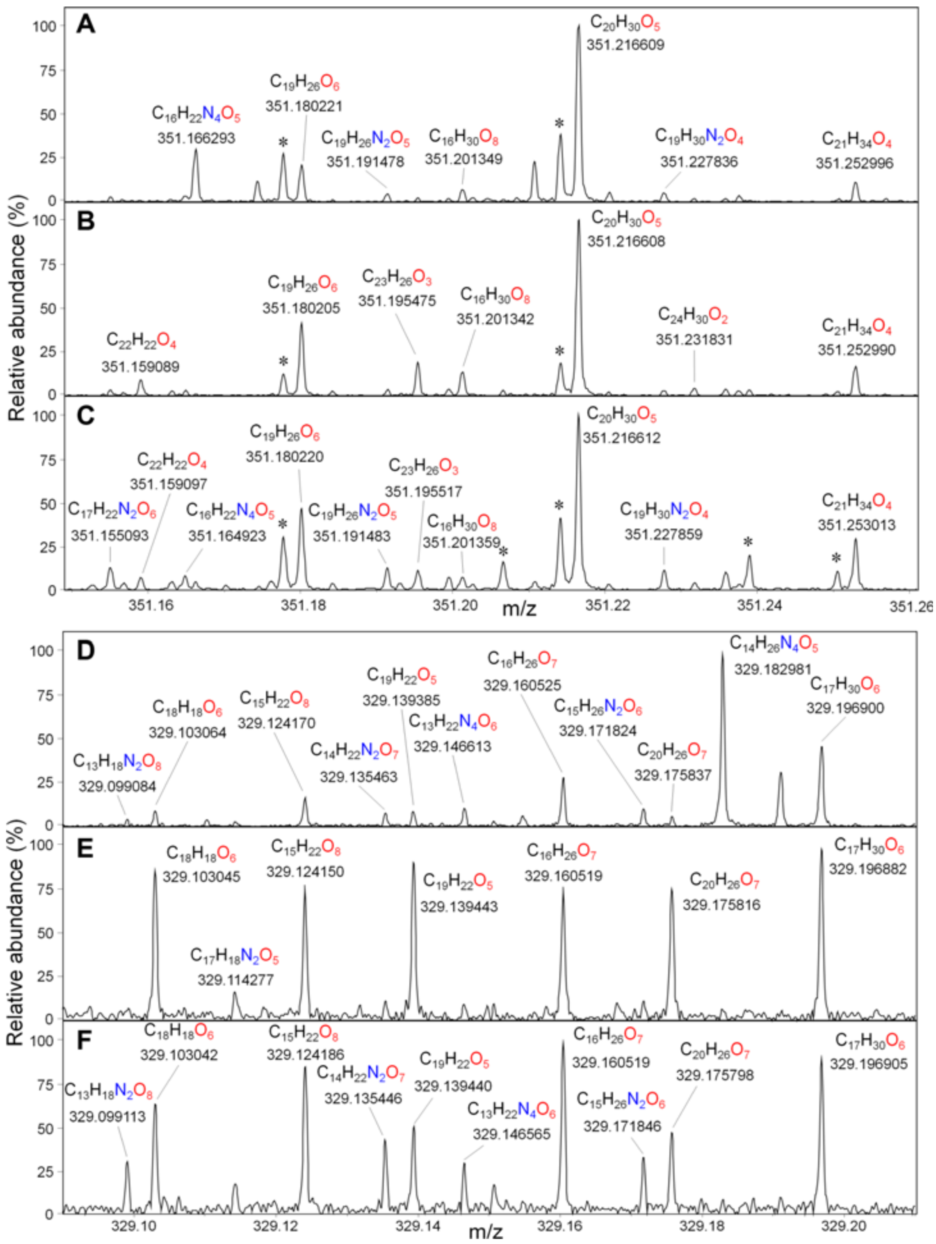

Fig. 7. Expanded ESI FTMS spectra of DOM for a nominal mass of m/z 351 (A-C) by positive ion mode and 329 (D-F) by negative ion mode: Oe (A and D), 2Oe1 (B and E), and 2A (C and F). The asterisks indicate the peaks observed in blank experiments.

availability at the deep organic layer and mineral layer in the permafrost upon permafrost thawing.

Major compound classes for the assigned chemical compositions (*i.e.*, lipids, proteins and amino sugars, carbohydrates, unsaturated hydrocarbons, condensed aromatics, lignins, and tannins) were displayed in the van Krevelen plots to provide compound information (Fig. 6), as previously demonstrated [27,37]. The van Krevelen diagram for the 2Oe1 horizon shows a more diverse distribution of organic compounds in comparison to the top soils (Oe horizon). In particular, the relative contents of lipids, lignins, tannins, and condensed aromatics compounds seemed significantly increased in the 2Oe1 and 2A horizons. The lignins, tannins and lipids class compounds were considered likely plant or microbal-derived products. The lignins and tannins-like compounds also have greater bioavailability, whereas the lipids have greater unavailability [38]. The increase in those compound contents in the deeper organic soils was much greater as compared to those in the surface soils. But the TC values were declined with soil depth in active layer so it might be possible that the increased aspects on the compound classes can be due to the decreased specific compound classes, resulting in the expansion of the apparent heterogeneity of the DOM.

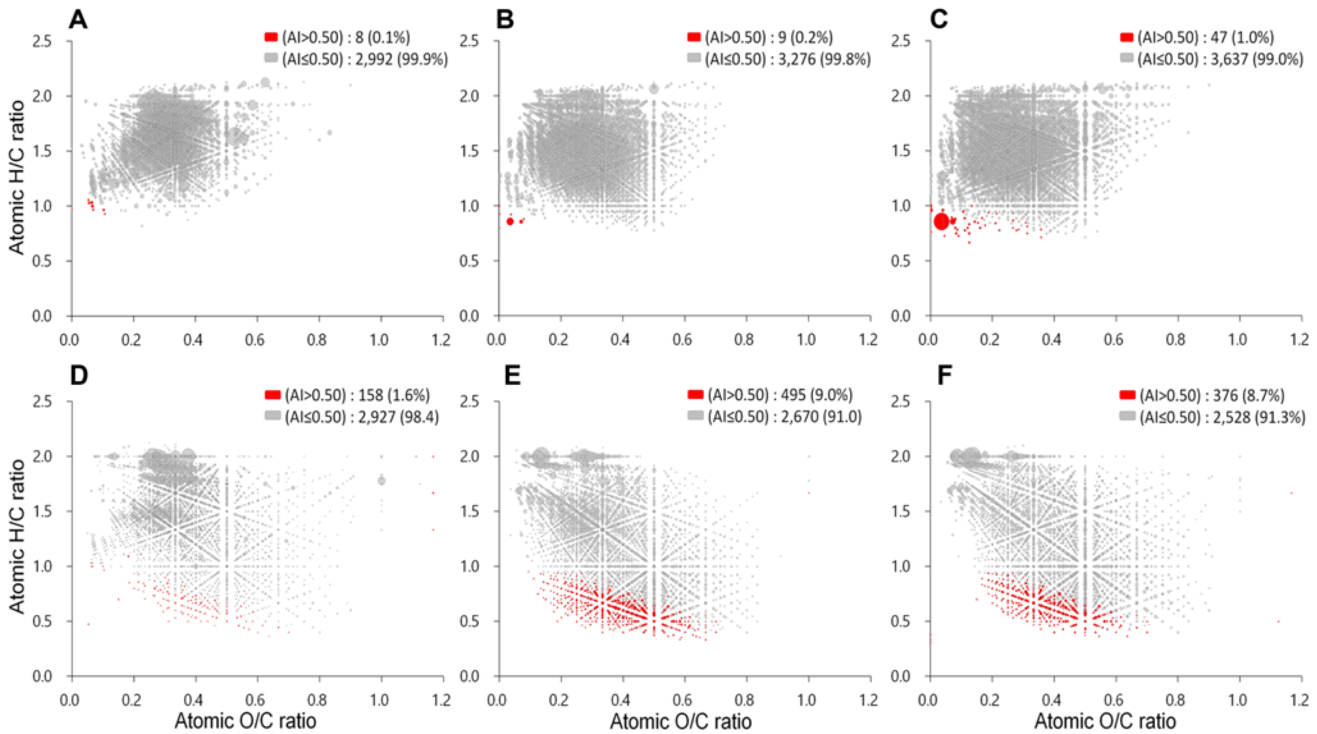

Fig. 8. Van Krevelen diagrams showing the molar H/C and O/C ratios with aromaticity index (AI) of assigned elemental compositions from arctic tundra soil extracts, analyzed by ESI (+) and (-) FT-ICR MS (color code: AI≤0.5, gray; AI>0.67, red). (A) Oe, (B) 2Oe1, and (C) 2A were analyzed *via* ESI (+), while (D) Oe, (E) 2Oe1, and (F) 2A were analyzed *via* ESI (-).

Among those compounds, the presence of aromatic molecules in soils is often used to be an indicative factor of the decomposability of SOM because the aromatic compounds are often considered a recalcitrant material owing to the resistance to decomposition. Aromaticity index (AI) proposed by Koch *et al.* [39] was employed to interpret the presence of aromatic structures in a molecule. The compounds with values of AI>0.5 are expected to be aromatic species. As displayed in Figs. 8D, 8E, and 8F, the Oe horizon appear to contain few aromatic compounds, but the 2Oe1 and 2A are, in total, composed of 9.0 and 8.7% aromatics, respectively. In comparison to the DOM MS spectra obtained *via* negative ion mode, the 2Oe1 and 2A with positive ion mass spectra appear to have less aromatic (0.2 and 1.0% of the total, respectively) structures (Figs. 8A, 8B, and 8C)), suggesting that the aromatic compounds might have acidic property probably owing to their hydroxyl groups. Balcarczyk *et al.* reported that the less aromatic compounds reflect the higher biodegradability of DOM [40], implying that the surface soil has undergone less decomposition and exhibits potentially higher decomposability, whereas the deeper organic soils have had more decomposition and resulted in the higher content of the recalcitrant materials.

Interestingly, the DOM profiles of the 2Oe1 horizon in active layer seemed more similar to those of the 2A horizon in permafrost each other, not the Oe horizon from the same active layer (Figs. 5 and 6). In particular, the declined content of CHON class species in the deep organic layer seemed a little bit increased in the permafrost layer. Permafrost usually preserves a stable environment, while active layer shows dynamically various ecological, and biogeochemical activities [41]. Recently, Ernakovich and coworkers demonstrated that the constituents of SOM can be utilized to differentiate the mineral and organic active layer soils, and suggested that the cryoturbation process, which has commonly observed in permafrost areas due to repeated freeze-thaw processes, resulting in mixing of soil layers [42,43], contributed to introducing SOM into the permafrost [44]. In addition, the leached DOM from upper soils by ice melt of frozen ground might be another contributor for the compositional diversity of DOM in the 2A horizon at the permafrost layer [45].

In this study, we demonstrated the different compositional profiles of arctic SOM in relation to the decomposability of DOM and the related factors. There may be much more significant factors contributing to that, and thus further consideration to the arctic soils is required to better understand permafrost changes associated with global warming and climate change.

4. Conclusion

The molecular characterization of DOM in moist acidic tussock tundra soils by a 15T FT-ICR mass spectrometer unveiled the detailed elemental compositions and class distributions of the compounds and provided insight into the SOM likely affecting the Arctic environments. According to the molecular profiles of DOMs depending on the soil depths in tundra permafrost, the decomposability of the permafrost DOM was demonstrated in this study. Although the analytical approach using ultra-high resolution FT-ICR MS cannot analyze mineral-associated OM in permafrost soils, it showed great potential as tools for obtaining compositional and structural information on DOM in arctic tundra soils, and this analysis is important for understanding permafrost changes associated with global warming and climate change.

Acknowledgements

This work was supported by grants from KBSI (G37110) and National Research Foundation of Korea funded by the Korean Government (NRF-2011-0021067) (PN15082).

Electronic Supplementary Material (ESM) The online version of this article (doi: 10.1007/s12257-017-0121-4) contains supplementary material, which is available to authorized users.

References

1. Oechel, W. C., S. J. Hastings, G. Vourlrtis, M. Jenkins, G. Riechers, and N. Grulke (1993) Recent change of Arctic tundra ecosystems from a net carbon dioxide sink to a source. *Nature* 361: 520-523.
2. Ping, C. L., G. J. Michaelson, M. T. Jorgenson, J. M. Kimble, H. Epstein, V. E. Romanovsky, and D. A. Walker (2008) High stocks of soil organic carbon in the North American Arctic region. *Nat. Geosci.* 1: 615-619.
3. Tarnocai, C., J. G. Canadell, E. A. G. Schuur, P. Kuhry, G. Mazhitova, and S. Zimov (2009) Soil organic carbon pools in the northern circumpolar permafrost region. *Global Biogeochem. Cycles* 23: GB2023.
4. Ward, C. P. and R. M. Cory (2015) Chemical composition of dissolved organic matter draining permafrost soils. *Geochim. Cosmochim. Acta* 167: 63-79.
5. Grosse, G., J. Harden, M. Turetsky, A. D. McGuire, P. Camill, C. Tarnocai, S. Frolking, E. A. G. Schuur, T. Jorgenson, S. Marchenko, V. Romanovsky, K. P. Wickland, N. French, M. Waldrop, L. Bourgeau-Chavez, and R. G. Striegl (2011) Vulnerability of high-latitude soil organic carbon in North America to disturbance. *J. Geophys. Res.* 116: G00K6.
6. Bardgett, R. D., C. Freeman, and N. J. Ostle (2008) Microbial contributions to climate change through carbon cycle feedbacks. *ISME J.* 2: 805-814.
7. Schuur, E. A., J. G. Vogel, K. G. Crummer, H. Lee, J. O. Sickman, and T. E. Osterkamp (2009) The effect of permafrost thaw on old carbon release and net carbon exchange from tundra. *Nature* 459: 556-559.
8. Powlson, D. S., P. R. Hirsch, and P. C. Brookes (2001) The role of soil microorganisms in soil organic matter conservation in the tropics. *Nutr. Cycl. Agroecosyst.* 61: 41-51.
9. Dunaj, S. J., J. J. Vallino, M. E. Hines, M. Gay, C. Kobyljanec, and J. N. Rooney-Varga (2012) Relationships between soil organic matter, nutrients, bacterial community structure, and the performance of microbial fuel cells. *Environ. Sci. Technol.* 46: 1914-1922.
10. Jastrow, J. D., R. M. Miller, and J. Lussenhop (1998) Contributions of interacting biological mechanisms to soil aggregate stabilization in restored prairie. *Soil Biol. Biochem.* 30: 905-916.
11. Chenu, C., C. Rumpel, and J. Lehmann (2015) *Methods for studying soil organic matter: Nature, dynamics, spatial accessibility, and interaction with minerals*. pp. 383-419 Academic Press, London, UK.
12. Kogel-Knabner, I. (2000) Analytical approaches for characterizing soil organic matter. *Org. Geochem.* 31: 609-625.
13. Beyer, L., C. Wachendorf, and C. Koebbemann (1993) A simple wet chemical extraction procedure to characterize soil organic matter (SOM). I. application and recovery rate. *Commun. Soil Sci. Plant Anal.* 24: 1645-1663.
14. Poirier, N., S. P. Sohi, J. L. Gaunt, N. Mahieu, E. W. Randall, D. S. Powlson, and R. P. Evershed (2005) The chemical composition of measurable soil organic matter pools. *Org. Geochem.* 36: 1174-1189.
15. Bonfleur, E. J., R. S. Kookana, V. L. Tornisielo, and J. B. Regitano (2016) Organomineral interactions and herbicide sorption in brazilian tropical and subtropical oxisols under no-tillage. *J. Agric Food Chem.* 64: 3925-3934.
16. Savini, M. C., R. M. Loewy, V. E. Nicotra, and M. E. Parolo (2017) Contribution of soil components on the sorption of chlorpyrifos. *Water Air Soil Pollut.* 228: 36.
17. Chen, W., P. Westerhoff, J. A. Leenheer, and K. Booksh (2003) Fluorescence excitation-emission matrix regional intergration to quantify spectra for dissolved organic matter. *Environ. Sci. Technol.* 37: 5701-5710.
18. De la Rosa, J. M., J. A. González-Pérez, R. González-Vázquez, H. Knicker, E. López-Capel, D. A. C. Manning, and F. J. González-Vila (2008) Use of pyrolysis/GC-MS combined with thermal analysis to monitor C and N changes in soil organic matter from a Mediterranean fire affected forest. *Catena* 74: 296-303.
19. Eshetu, B., G. Jandl, and P. Leinweber (2012) Compost changed soil organic matter molecular composition: A Py-GC/MS and Py-FIMS study. *Compost. Sci. Util.* 20: 230-238.
20. Cho, Y., A. Ahmed, A. Islam, and S. Kim (2015) Developments in FT-ICR MS instrumentation, ionization techniques, and data interpretation methods for petroleomics. *Mass Spectrom Rev.* 34: 248-263.
21. Mazur, D. M., M. Harir, P. Schmitt-Kopplin, O. V. Polyakova, and A. T. Lebedev (2016) High field FT-ICR mass spectrometry for molecular characterization of snow board from Moscow regions. *Sci. Total Environ.* 557-558: 12-19.
22. Ksionzek, K. B., O. J. Lechtenfeld, S. L. McCallister, P. Schmitt-Kopplin, J. K. Geuer, W. Geibert, and B. P. Koch (2016) Dissolved organic sulfur in the ocean: Biogeochemistry of a petagram inventory. *Science* 354: 456-459.
23. Guigue, J., M. Harir, O. Mathieu, M. Lucio, L. Ranjard, J. Lévêque, and P. Schmitt-Kopplin (2016) Ultrahigh-resolution FT-ICR mass spectrometry for molecular characterisation of pressurised hot water-extractable organic matter in soils. *Biogeochem.* 128: 307-326.

24. Lobodin, V. V., P. Juyal, A. M. McKenna, R. P. Rodgers, and A. G. Marshall (2014) Lithium cationization for petroleum analysis by positive ion electrospray ionization Fourier transform ion cyclotron resonance mass spectrometry. *Energy and Fuels* 28: 6841-6847.
25. Antony, R., A. M. Grannas, A. S. Willoughby, R. L. Sleighter, M. Thamban, and P. G. Hatcher (2014) Origin and sources of dissolved organic matter in snow on the East Antarctic ice sheet. *Environ. Sci. Technol.* 48: 6151-6159.
26. Wu, Z., R. P. Rodgers, and A. G. Marshall (2004) Two- and three-dimensional van krevelen diagrams: A graphical analysis complementary to the kendrick mass plot for sorting elemental compositions of complex organic mixtures based on ultrahigh-resolution broadband fourier transform ion cyclotron resonance mass measurements. *Anal. Chem.* 76: 2511-2516.
27. Kim, S., R. W. Kramer, and P. G. Hatcher (2003) Graphical method for analysis of ultrahigh-resolution broadband mass spectra of natural organic matter, the van Krevelen diagram. *Anal. Chem.* 75: 5336-5344.
28. Mann, B. F., H. Chen, E. M. Herndon, R. K. Chu, N. Tolic, E. F. Portier, T. Roy Chowdhury, E. W. Robinson, S. J. Callister, S. D. Wullschleger, D. E. Graham, L. Liang, and B. Gu (2015) Indexing permafrost soil organic matter degradation using high-resolution mass spectrometry. *PLoS One* 10: e0130557.
29. Hobbie, S. E., T. A. Miley, and M. S. Weiss (2002) Carbon and nitrogen cycling in soils from acidic and nonacidic tundra with different glacial histories in northern Alaska. *Ecosystems* 5: 761-774.
30. Hobbie, S. E. and L. Gough (2004) Litter decomposition in moist acidic and non-acidic tundra with different glacial histories. *Oecologia* 140: 113-124.
31. Ricketts, M. P., R. S. Poretsky, J. M. Welker, and M. A. Gonzalez-Meler (2016) Soil bacterial community and functional shifts in response to altered snowpack in moist acidic tundra of northern Alaska. *Soil* 2: 459-474.
32. Kim, H. (2016) *Study on prokaryotic community structure in moist acidic tundra soil in Council, Alaska.* Ph. D. Thesis. Seoul National University, Seoul, Republic of Korea.
33. Choi, J. H., J. Ryu, S. Jeon, J. Seo, Y. H. Yang, S. P. Pack, S. Choung, and K. S. Jang (2017) In-depth compositional analysis of water-soluble and -insoluble organic substances in fine (PM2.5) airborne particles using ultra-high-resolution 15T FT-ICR MS and GC×GC-TOFMS. *Environ. Pollut.* 225: 329-337.
34. Mazzoleni, L. R., B. M. Ehrmann, X. Shen, A. G. Marshall, and J. L. Collett, Jr. (2010) Water-soluble atmospheric organic matter in fog: Exact masses and chemical formula identification by ultrahigh-resolution fourier transform ion cyclotron resonance mass spectrometry. *Environ. Sci. Technol.* 44: 3690-3697.
35. Koch, B. P., M. R. Witt, R. Engbrodt, T. Dittmar, and G. Kattner (2005) Molecular formulae of marine and terrigenous dissolved organic matter detected by electrospray ionization fourier transform ion cyclotron resonance mass spectrometry. *Geochim. Cosmochim. Acta* 69: 3299-3308.
36. D'Andrilli, J., T. Dittmar, B. P. Koch, J. M. Purcell, A. G. Marshall, and W. T. Cooper (2010) Comprehensive characterization of marine dissolved organic matter by Fourier transform ion cyclotron resonance mass spectrometry with electrospray and atmospheric pressure photoionization. *Rapid Commun. Mass Spectrom.* 24: 643-650.
37. Wozniak, A. S., J. E. Bauer, R. L. Sleighter, R. M. Dickhut, and P. G. Hatcher (2008) Technical Note: Molecular characterization of aerosol-derived water soluble organic carbon using ultrahigh resolution electrospray ionization Fourier transform ion cyclotron resonance mass spectrometry. *Atmos. Chem. Phys.* 8: 5099-5111.
38. Ohno, T., T. B. Parr, M. C. Gruselle, I. J. Fernandez, R. L. Sleighter, and P. G. Hatcher (2014) Molecular composition and biodegradability of soil organic matter: A case study comparing two new England forest types. *Environ. Sci. Technol.* 48: 7229-7236.
39. Koch, B. P. and T. Dittmar (2006) From mass to structure: An aromaticity index for high-resolution mass data of natural organic matter. *Rapid Commun. Mass Spectrom.* 20: 926-932.
40. Balcarczyk, K. L. and J. B. Jones Jr. (2009) Stream dissolved organic matter bioavailability and composition in watersheds underlain with discontinuous permafrost. *Biogeochem.* 94: 255-270.
41. Kane, D. L., L. D. Hinzman, and J. P. Zarling (1991) Thermal response of the active layer to climatic warming in a permafrost environment. *Cold Reg. Sci. Tech.* 19: 111-122.
42. Bockheim, J. G. and C. Tarnocai (1998) Recognition of cryoturbation for classifying permafrost-affected soils. *Geoderma.* 81: 281-293.
43. Kaiser, C., H. Meyer, C. Biasi, O. Rusalimova, P. Barsukov, and A. Richter (2007) Conservation of soil organic matter through cryoturbation in arctic soils in Siberia. *J Geophys. Res.* 112: G02017.
44. Ernakovich, J. G., M. D. Wallenstein, and F. J. Calderon (2015) Chemical indicators of cryoturbation and microbial processing throughout an Alaskan permafrost soil depth profile. *Soil Sci. Soc. Am. J.* 79: 783-793.
45. Grosse, G., J. W. Harden, M. Turetsky, A. D. McGuire, P. Camill, C. Tarnocai, S. Frolking, E. A. G. Schuur, T. Jorgenson, S. Marchenko, V. Romanovsky, K. P. Wickland, N. French, M. Waldrop, L. Bourgeau-Chavez, and R. G. Strigl (2011) Vulnerability of high-latitude soil organic carbon in North America to disturbance. *J. Geophys. Res.* 116: G00K6.
46. Staff, S. S. (2014) *Keys to Soil Taxonomy.* USDA-Natural Resources Conservation Service, Washington DC, USA.